



**HAL**  
open science

## Electrooptical properties of rubidium hydrogen selenate

Jean-Paul Salvestrini, L. Guilbert, M. D. Fontana, Z. Czapla

► **To cite this version:**

Jean-Paul Salvestrini, L. Guilbert, M. D. Fontana, Z. Czapla. Electrooptical properties of rubidium hydrogen selenate. *Journal of the Optical Society of America B*, 1997, 14 (11), pp.2818-2822. <10.1364/JOSAB.14.002818>. <hal-00186050>

**HAL Id: hal-00186050**

**<https://hal.science/hal-00186050v1>**

Submitted on 3 Dec 2021

HAL is a multi-disciplinary open access archive for the deposit and dissemination of scientific research documents, whether they are published or not. The documents may come from teaching and research institutions in France or abroad, or from public or private research centers.

L'archive ouverte pluridisciplinaire HAL, est destinée au dépôt et à la diffusion de documents scientifiques de niveau recherche, publiés ou non, émanant des établissements d'enseignement et de recherche français ou étrangers, des laboratoires publics ou privés.



Distributed under a Creative Commons CC BY-NC 4.0 - Attribution - Non-commercial use - International License

# Electro-optical properties of rubidium hydrogen selenate: influence of the dc electric field and origin of the large electro-optic coefficient

J. P. Salvestrini, L. Guilbert, and M. D. Fontana

*Laboratoire Matériaux Optiques à Propriétés Spécifiques, Centre Lorrain d'Optique et d'Electronique des Solides, Université de Metz et Supelec 2, rue E. Belin 57078 Metz Cedex 3, France*

Z. Czapla

*Institute of Experimental Physics, University of Wrocław, Place Maxa Borna 9, 50-205 Wrocław, Poland*

Rubidium hydrogen selenate (RbHSeO<sub>4</sub>) was recently reported as exhibiting one of the largest electro-optic coefficients ever measured in any material. We report on the dependence of the electro-optic properties on the dc electric field. This behavior can be interpreted by the change in the birefringence that is due to the domain reversal. This particular electro-optic effect also explains the large sensitivity of the electro-optical properties to the orientation of the laser beam-propagation direction with respect to the domain walls.

*Key words:* Electro-optical materials, RbHSeO<sub>4</sub>, ferroelectric, domains.

## 1. INTRODUCTION

Rubidium hydrogen selenate [RbHSeO<sub>4</sub> (RHSe)] displays ferroelectric and ferroelastic properties at room temperature<sup>1</sup> and has recently attracted a special interest owing to its large electro-optic (EO) properties. We have indeed measured an EO coefficient equal to 13500 pm/V when a dc voltage is applied on a single crystal.<sup>2</sup> This renders RHSe as a promising material for the modulation of a laser beam since the half-wave voltage could be a few volts. Furthermore, we have noted the large remanent birefringence when the electric field is removed, which could lead to a shift in the working point of the EO modulator and thus should limit the possibilities for analogic applications.

In this paper we are concerned with the origin of the large EO properties of RHSe under a dc field. For this, we recorded birefringence cycles and capacity cycles on different samples, and, particularly, we studied the influence of the beam direction on the shape of the birefringence cycle. The role of the domain structure in this special EO effect presented by the RHSe is pointed out. All the results are interpreted within a simple model built on the domain reversal and the subsequent birefringence variations under a dc field.

## 2. EXPERIMENT

The RHSe crystal displays triclinic symmetry at room temperature with pseudo-orthorhombic lattice parameters.<sup>1</sup> The investigation of the electro-optic properties in triclinic crystals is not simple since, in principle, all the components of the electro-optic tensor are allowed.

For this study, we were especially interested in the effective EO coefficient  $r_b = r_{12} - (n_2^2/n_1^2)r_{22}$ . This coef-

ficient can be obtained when one measures the electric-field-induced birefringence or the corresponding phase shift  $\Gamma$  when the laser beam is propagated along the  $z$  axis and dc voltage is applied along the  $y$  axis. Here,  $x$ ,  $y$ , and  $z$  refer to the pseudo-orthorhombic system axes. We thus determine the EO coefficient from the following equation:

$$r_b = \frac{\lambda d}{\pi L n_1^3} \frac{\Gamma}{V} \quad (1)$$

where  $d$  is the interelectrode spacing,  $L$  is the crystal length along the laser beam-propagation direction,  $\lambda$  is the wavelength of the light, and  $V$  is the applied voltage.

For the measurement of the phase shift induced by a dc electric field, we used the experimental Sénarmont set up.<sup>3</sup> The optical transmission of such a system, which is drawn schematically in Fig. 1, follows the general law

$$\frac{I}{I_0} = \frac{1}{2} [1 - \sin(\Gamma - 2\beta)] \quad (2)$$

if the optical absorption is neglected. In this equation,  $I_0$  and  $I$  are, respectively, the input and output laser intensity, and  $\Gamma$  is the total phase shift introduced by the sample.  $\Gamma$  is due to the natural birefringence of the crystal and to its variations induced by the temperature, by an electric field, or by a mechanical strain.  $\Gamma$  can be compensated by an adjustment of the angle  $\beta$  of the analyzer. We applied dc and ac voltages to the crystal, and thus the phase retardation  $\Gamma$  could include the static component  $\Gamma^*$  owing to the spontaneous birefringence of the crystal

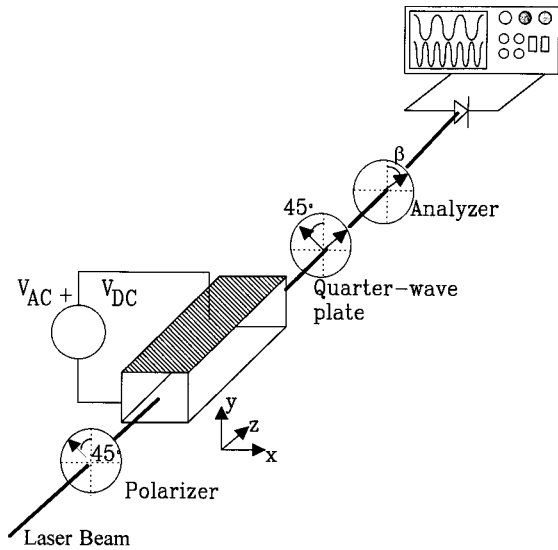


Fig. 1. Basic arrangement of the optical and the electronic components in the Sénarmont setup employed in this study. The axes of the polarizer and the quarter-wave plate are at  $45^\circ$  of the neutral lines of the crystal. The dc and the ac electric fields are applied to the crystal along the  $y$  axis. When  $\beta = \beta_0 = (\Gamma^*/2) - (\pi/4) + k\pi$ ,  $k = 0, 1, 2, \dots$ , the frequency of the output signal is twice the frequency of the applied ac electric field.

and to the applied dc field together with a dynamic component,  $\Gamma_m \sin(\omega_m t)$ , which is due to the applied ac field at the pulsation  $\omega_m = 2\pi f$ . Thus if

$$E = E_{dc} + E_{ac} = E_{dc} + E_m \sin(2\pi f t), \quad (3)$$

$\Gamma$  is expressed as

$$\Gamma = \Gamma(0) + \Gamma_{dc} + \Gamma_m \sin(2\pi f t) = \Gamma^* + \Gamma_m \sin(2\pi f t). \quad (4)$$

If we adjust the angle of the analyzer to the value  $\beta$ ,

$$\beta = \beta_0 = \frac{\Gamma^*}{2} - \frac{\pi}{4} + k\pi, \quad k = 0, 1, 2, \dots, \quad (5)$$

the harmonic study by Bessel's functions of Eq. (2) shows that the dc intensity transmitted is minimum and only the ac component at double frequency  $f' = 2f$  survives in the modulated intensity output with an amplitude of

$$J_{2f} = \frac{I_0}{8} \Gamma_m^2 \left( 1 - \frac{\Gamma_m^2}{12} \right). \quad (6)$$

As shown in a previous paper,<sup>4</sup> a sharp and clear frequency doubling appears on the monitoring oscilloscope screen. We deduce the EO phase retardation by the difference between two values of  $\beta$  obtained successively without and with a dc electric field:

$$\Gamma(E) = 2[\beta_0 - \beta_0(0)] = 2\beta_0(E). \quad (7)$$

$\beta_0(0)$  thus corresponds to the analyzer angle compensating the phase shift owing to the natural birefringence of the crystal ( $E = 0$ ). Our method basically differs from the other techniques that are usually employed for EO measurements because it yields the direct determination of the phase shift when the azimuthal angle on the goniometric circle of the analyzer is read.

This method is very sensitive and leads to a large accuracy for the measurements of the phase shift with an absolute error of  $\pm 1^\circ$  in  $\Gamma$ . Nevertheless, several secondary effects can induce error during the measurement of  $\beta$ . Within this method and before applying a dc field, the analyzer angle  $\beta$  is adjusted to compensate the natural phase shift  $\Gamma(0)$  related to  $\Delta n(0)$ . Consequently, only the electric-field-induced phase shift  $\Gamma(E)$  is in principle measured. In fact,  $\Gamma(0)$  can vary with temperature during the measurements. Therefore this dependence of  $\Gamma(0)$  is determined by the application of only the ac voltage on the sample. In RHSe, we obtained a variation of the phase shift  $\Delta\Gamma$  owing to a temperature shift  $\Delta T$  equal to  $12^\circ/\text{K}$  for the longest sample. As the temperature was controlled within  $\pm 0.1$  K, we accounted for an error of  $\pm 1.2^\circ$  owing to temperature change during measurements. The total error in  $\Gamma$  of our measurements were thus equal to  $\pm 2.2^\circ$ .

Our measurements were carried out with a 20-mW He-Ne laser at  $6328 \text{ \AA}$ . The observation of the output is achieved on an oscilloscope screen, and the azimuthal angles of the analyzer, corresponding to the different values of  $\beta_0$ , are given by the  $0.01^\circ$  stepping-motor driver. The measurements were performed on three samples of respective dimensions:  $7.49 \text{ mm} \times 3.02 \text{ mm} \times 1.88 \text{ mm}$ ,  $6.10 \text{ mm} \times 2.55 \text{ mm} \times 2 \text{ mm}$ , and  $8.90 \text{ mm} \times 3.07 \text{ mm} \times 2 \text{ mm}$ . Dielectric measurements were performed on the same RHSe samples as used for EO experiments by means of a Sawyer-Tower bridge. The relative error on the capacity measurements (and thus on the deduced permittivity) is typically 10%.

### 3. EXPERIMENTAL RESULTS

The EO coefficients can be determined from the variation of the birefringence  $\Delta n$ , which is induced by the electric field  $E$ . Figure 2 shows the behavior of the phase shift

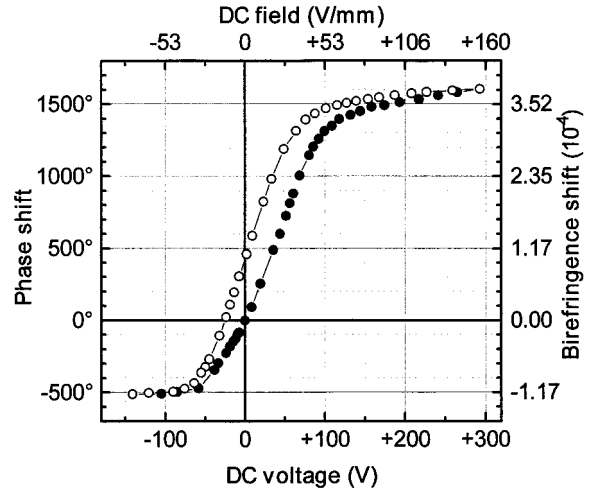


Fig. 2. Phase shift  $\Gamma$  induced in a  $7.49 \text{ mm} \times 3.02 \text{ mm} \times 1.88 \text{ mm}$  sample of RHSe by a dc voltage (filled circles represent increasing voltage; open circles represent decreasing voltage) for the 633-nm wavelength of a He-Ne laser. The propagation of the laser beam was along a direction at approximately  $3^\circ$  with respect to the  $z$  axis in the  $(y, z)$  plane, and the electric field was applied along the ferroelectric  $y$  axis. The axes  $x$ ,  $y$ , and  $z$  refer to the pseudo-orthorhombic system.

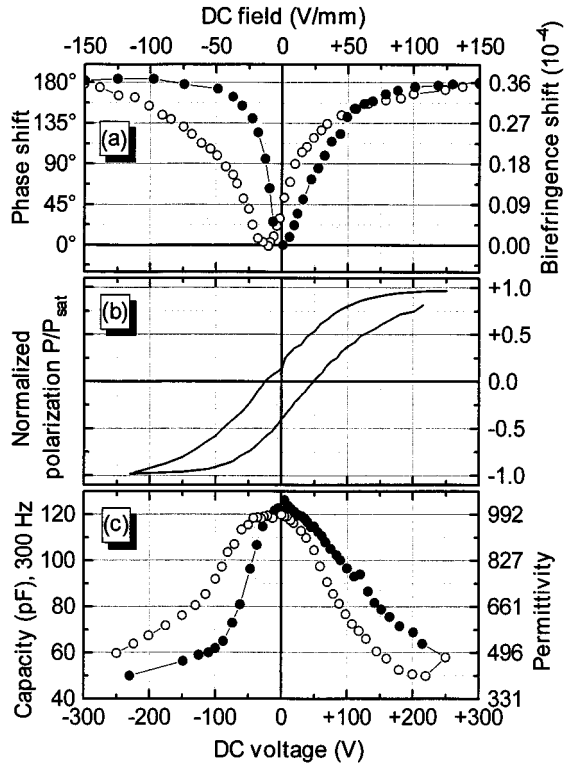


Fig. 3. Comparison between the cycles displayed by (a) the birefringence, (b) the polarization, and (c) the dielectric permittivity as a function of dc voltage in a  $8.61 \text{ mm} \times 3.1 \text{ mm} \times 1.95 \text{ mm}$  RHTe sample (filled circles represent increasing voltage; open circles represent decreasing voltage). The left-hand axes correspond to the measured quantity (i.e., phase shift and capacity), whereas the right-hand axes yield the quantities  $\Delta n$  and  $\epsilon$ , which are independent of the sample dimensions and are more convenient as physical parameters. The total recording time was approximately 3 hours (loop frequency  $10^{-4}$  Hz). The laser beam (633 nm) was propagated exactly along the  $z$  axis of the crystal, and the electric field was applied along the  $y$  axis (ferroelectric axis). The plot  $P(E)/P_s$  is deduced by integration from the experimental capacity cycle and is normalized to unity.

with both increasing and decreasing dc voltage. The linear part of the curve yields the EO Pockels coefficient  $r_b$ , which is here exceptionally large ( $n^3 r_b = 13500 \text{ pm/V}$ ), as reported earlier.<sup>2</sup>

Here we are dealing with the complete dependence of the curve  $\Delta n$  versus  $E$ . The shape obtained looks like the hysteresis loop  $P(E)$  shown by the polarization induced by the electric field in ferroelectric materials. In these compounds, antiparallel ferroelectric domains can be associated with the values  $+P_s$  or  $-P_s$  of the spontaneous polarization. We recall that  $P_s$ , or domains, can be reversed under the application of an electric field, leading to a change in optical properties. Therefore we attempt to relate the behavior of  $\Delta n(E)$  with the ferroelectric properties of RHTe. We consequently undertake simultaneous measurements of the birefringence and the dielectric permittivity as a function of the dc field  $E$ . For this, we prepare two crystals with faces having an orientation that is different with respect to the domain walls. If  $\theta$  refers to the angle between the direction of the propagating beam and the  $z$  axis in the  $(x, z)$  plane, the first sample is cut to have  $\theta$  exactly equal to zero, whereas the second crystal is prepared with  $\theta$  equal to  $21^\circ$ .

Figures 3 and 4 exhibit both the cycle of the phase shift  $\Gamma$  (or the induced birefringence) and the capacity (or the dielectric permittivity) recorded for the two samples (with  $\theta = 0^\circ$  and  $\theta = 21^\circ$ ). The curves  $P(E)$ , as derived from the integration of the permittivity, are also plotted for comparison. The plot  $\Delta n(E)$  shows a symmetric (or nearly symmetric) and quadratic shape in the first case (sample  $\theta = 0^\circ$ ; Fig. 3) but an antisymmetric shape in the second case (sample  $\theta = 21^\circ$ ; Fig. 4). This means that the cycle of the birefringence is much affected by the value of the incidence angle  $\theta$ .

For the sample with  $\theta = 21^\circ$  we note the similarities between curves  $\Delta n(E)$  and  $P(E)$ . In this case, the electric field needed to reverse each saturated state, i.e., the so-called coercive field, is remarkably low (20 V/mm). This switching is accompanied by a very large change in the birefringence (more than  $10^{-3}$ ). As a consequence, the slope in the linear part of  $\Delta n(E)$  is very large and the quasi-static ( $10^{-4}$  Hz) value of the effective EO coefficient is huge ( $n^3 r_{\text{eff}} \sim 100000 \text{ pm/V}$ ).

Note that the asymmetric cycle reported in Fig. 2 was obtained for an incidence angle  $\theta \approx 3^\circ$  in the  $(y, z)$

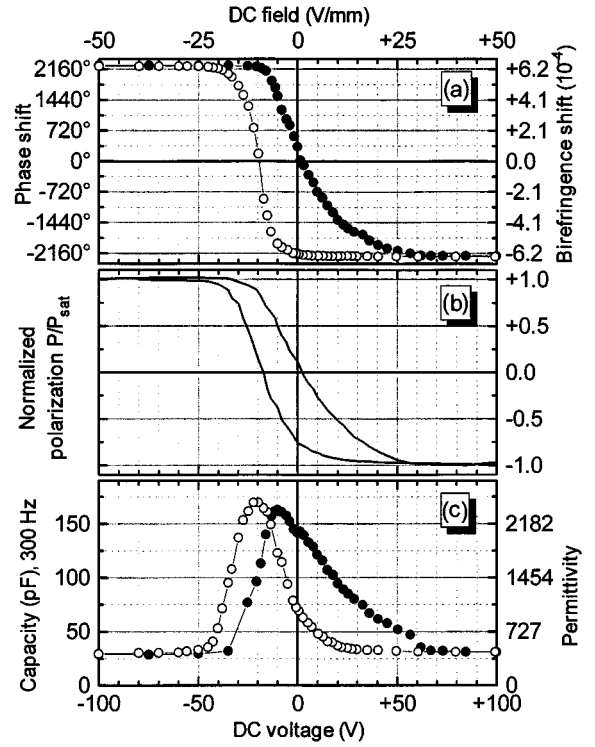


Fig. 4. Comparison between the cycles displayed by (a) the birefringence, (b) the polarization, and (c) the dielectric permittivity as a function of dc voltage, in a  $6.1 \text{ mm} \times 2.55 \text{ mm} \times 2 \text{ mm}$  RHTe sample (filled circles represent increasing voltage; open circles represent decreasing voltage). The left-hand axes correspond to the measured quantity (i.e., phase shift and capacity), whereas the right-hand axes yield the quantities  $\Delta n$  and  $\epsilon$ , which are independent of the sample dimensions and are more convenient as physical parameters. The total recording time was approximately 3 hours (loop frequency  $\approx 10^{-4}$  Hz). The laser beam (633 nm) was propagated along a direction at  $21^\circ$  with respect to the  $z$  axis of the crystal, and the electric field was applied along the ferroelectric  $y$  axis. The plot  $P(E)/P_s$  is deduced by integration from the experimental capacity cycle and is normalized to unity.

plane. This shape corresponds to an intermediate situation between the two other cycles.

#### 4. INTERPRETATION

At room temperature, RHSe is in a ferroelectric-ferroelastic phase. This phase exhibits a layered domain structure with domain walls parallel to the (001) crystallographic planes and a spontaneous polarization  $P_s$  oriented along the  $y$  axis.<sup>5</sup> Neighboring domains are symmetrical to each other by a twofold rotation around the  $z$  axis. This domain structure can be considered as especially soft at room temperature, since it can be easily reversed by the application of mechanical stresses or an electric field, and it reappears spontaneously as soon as the field is released after saturation.<sup>6</sup>

Another property of RHSe, first evidenced by Tsukamoto,<sup>6</sup> lies in the mutual tilt of the optical indicatrices in opposite domains as shown in Fig. 5. This feature, like in any ferroelastic domain structure, gives rise to a deflection phenomenon of the light. It results from reflection and refraction processes at domain walls from high index to low index or vice versa. The tilt of the indicatrices induces, in fact, a difference of birefringence between neighboring domains. Note that, for a light beam propagating exactly along the  $z$  axis, and which is perpendicular to the domain wall, the deflection process disappears and the difference of birefringence is exactly zero.

In light of these two properties of RHSe, the soft behavior of the domain structure, and the difference of birefringence between opposite domains, we attempted to interpret the origin of the large EO effect and thus the different shapes of the birefringence cycles that were obtained.

The phase shift caused by the birefringence through a crystal of thickness  $L$  along the direction of propagation is expressed as

$$\Gamma = \frac{2\pi}{\lambda} L \Delta n, \quad (8)$$

where  $\lambda$  is the laser wavelength and  $\Delta n$  is the (natural and/or induced) birefringence. Owing to the existence of domains polarized in opposite directions, denoted + and -,  $\Delta n$  is, in fact, the average birefringence, which can be written as

$$\Delta n = \frac{L^+}{L} \Delta n^+ + \frac{L^-}{L} \Delta n^-, \quad (9)$$

where  $L^+$  and  $L^-$  are the thicknesses of domains + and - respectively, and  $\Delta n^+$  and  $\Delta n^-$  are the respective birefringences (Fig. 5). These two quantities are different because of the mutual tilt of the indicatrices in neighboring domains.  $L = L^+ + L^-$  is the total thickness of the multidomain sample. The ferroelectric polarization  $P(E)$  results from the average of the spontaneous polarizations  $\pm P_s$  across the domain structure:

$$P(E) = P_s \left( \frac{L^+ - L^-}{L} \right). \quad (10)$$

The application of the electric field  $E$  on the crystal along the ferroelectric  $y$  axis leads to a change in the statistics

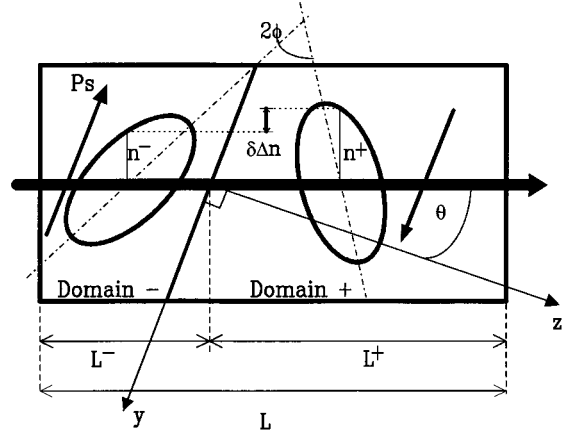


Fig. 5. Indicatrix cross sections in neighboring domains of RHSe in the  $(y, z)$  plane (the tilt angle  $\phi$  is voluntarily exaggerated). The tilt gives rise to a difference of birefringence between opposite domains, provided that the propagation direction is not perpendicular to the domain walls.

of domains + or -. When Eq. (10) is reversed, the ratios  $L^+/L$  and  $L^-/L$  can be expressed in terms of the average polarization  $P(E)$  of the sample

$$\frac{L^+}{L} = \frac{1}{2} \left( 1 + \frac{P(E)}{P_s} \right); \quad \frac{L^-}{L} = \frac{1}{2} \left( 1 - \frac{P(E)}{P_s} \right). \quad (11)$$

Substituting these expressions into Eq. (9), we get the electric-field dependence of the average birefringence:

$$\Delta n(E) = \Delta n_0 + \frac{1}{2} \delta \Delta n \frac{P(E)}{P_s}, \quad (12)$$

where  $\Delta n_0 = (\Delta n^+ + \Delta n^-)/2$ , and  $\delta \Delta n = \Delta n^+ - \Delta n^-$  is the difference of birefringence between opposite domains.

One expects from Eq. (12) that the birefringence should be proportional to the polarization  $P(E)$ , provided that the difference of birefringence  $\delta \Delta n$  is not zero. This quantity is directly determined by the variation of birefringence between the two saturated states of the birefringence cycle that correspond to  $P(E) = \pm P_s$ , according to Eq. (12).

For the sample with orientation  $\theta = 21^\circ$ , we get  $\delta \Delta n = 12.5 \times 10^{-4}$  in the cycle  $\Delta n(E)$ . Consequently, the behavior of  $\Delta n(E)$  has to reproduce the dependence of  $P(E)$ . This is clearly verified by the experimental data reported in Fig. 4. This relationship between  $\Delta n(E)$  and  $P(E)$  is corroborated by the two coercive states that occur at the same values of the dc electric field in both optical and polarization cycles.

In the crystal with  $\theta = 0^\circ$ , the incident beam is exactly normal to the (001) face of the crystal and thus to the domain walls so that  $\delta \Delta n$  is obviously equal to zero since the indicatrices in neighboring domains are symmetrical to each other with respect to the propagation direction (Fig. 5). Thus according to Eq. (12), the birefringence should be independent of the field, and the cycle should be absolutely flat. We checked experimentally (Fig. 3) that the difference of birefringence between the two saturated states is zero. However, the birefringence cycle shows a significant dependence on the electric field. The total

amplitude of the cycle, which is nevertheless much lower than in the other sample ( $0.36 \times 10^{-4}$  compared with  $12.5 \times 10^{-4}$ ), can be attributed to a second-order contribution caused by the ferroelastic strains that induce small changes of the incidence angle itself during the cycle. Thus, in this case, the birefringence cycle  $\Delta n(E)$  should be proportional to the square of the ferroelectric cycle  $P(E)$ , and the shape is expected to be symmetrical. This is verified in the experimental data of Fig. 3.

We can therefore re-express the average birefringence [Eq. (12)] in a more general form as

$$\Delta n(E) = \Delta n_0 + A \frac{P(E)}{P_s} + B \left[ \frac{P(E)}{P_s} \right]^2 + \dots \quad (13)$$

The sample with  $\theta = 0^\circ$  corresponds to the situation where  $A = 0$  and  $B \neq 0$ , whereas the sample with large incidence angle ( $\theta = 21^\circ$ ) is described by  $A \neq 0$  and  $B = 0$ . For samples with small angles  $\theta$ , an intermediate situation is expected ( $A \approx B \neq 0$ ) so that the birefringence cycle is neither symmetrical (quadratic) nor anti-symmetrical, as shown in Fig. 2.

## 5. CONCLUSION

By means of simultaneous measurements of the birefringence cycle and the dielectric permittivity under the dc field, we have pointed out that the huge EO properties of RHSe are due to an unusual phenomenon related to the large difference of the birefringence between two adjacent domains and to the progressive reversal of the ferroelectric domains under the dc field. We could thus explain

why the field-induced birefringence is strongly dependent on the angle between the propagating beam direction and the domain walls.

## ACKNOWLEDGMENTS

This work was supported by grant 6563 from the Komitet Badań Naukowych and the Ministère des Affaires Étrangères in the frame of the Polish–French scientific exchanges.

## REFERENCES

1. A. Waskowska, S. Olejnik, K. Lukaszewicz, and T. Glowiak, “Rubidium hydrogenselenate,” *Acta Crystallogr., Sect. B* **34**, 3344 (1978).
2. J. P. Salvestrini, M. D. Fontana, M. Aillerie, and Z. Czaplak, “New material with strong electro-optic effect: rubidium hydrogen selenate ( $\text{RbHSeO}_4$ ),” *Appl. Phys. Lett.* **64**, 1920 (1994).
3. M. Aillerie, M. D. Fontana, F. Abdi, C. Carabatos-Nedelec, and N. Theofanous, “Accurate measurement of the electrooptic coefficients: applications to  $\text{LiNbO}_3$ ,” *J. Soc. Photo-Opt. Instrum. Eng.* **94**, 1018 (1988).
4. F. Abdi, M. Aillerie, and M. D. Fontana, “Accurate measurements of the electrooptical properties of iron doped and pure  $\text{BaTiO}_3$  single crystals,” *Nonlinear Opt.* **16**, 65 (1996).
5. S. Suzuki, T. Osaka, and Y. Makita, “Successive phase transitions in ferroelectric  $\text{RbHSeO}_4$ ,” *J. Phys. Soc. Jpn.* **47**, 1741 (1979).
6. T. Tsukamoto, M. Komukae, S. Suzuki, H. Futama, and Y. Makita, “Domain structure and deflection of light at domain walls in  $\text{RbHSeO}_4$ ,” *J. Phys. Soc. Jpn.* **52**, 3966 (1983).